Materials Letters 89 (2012) 51–54

Contents lists available at SciVerse ScienceDirect

Materials Letters

journal homepage: www.elsevier.com/locate/matlet

In vitro corrosion inhibition on biomedical shape memory alloy by plasma-polymerized allylamine film

Penghui Li [a], Guosong Wu [a], Ruizhen Xu [a], Wenhao Wang [a,b], Shuilin Wu [a,c], Kelvin W.K. Yeung [b], Paul K. Chu [a,*]

[a] Department of Physics and Materials Science, City University of Hong Kong, Tat Chee Avenue, Kowloon, Hong Kong, China
[b] Division of Spine Surgery, Department of Orthopaedics and Traumatology, The University of Hong Kong, Pokfulam, Hong Kong, China
[c] College of Materials Science and Engineering, Hubei University, Wuhan 430062, China

ARTICLE INFO

Article history:
Received 12 June 2012
Accepted 16 August 2012
Available online 27 August 2012

Keywords:
NiTi
Plasma polymerization
Polymer film
Corrosion

ABSTRACT

To improve the corrosion resistance of biomedical nickel titanium (NiTi) alloy, a polymeric allylamine film is deposited by plasma polymerization. The chemical composition, surface morphology, and thickness of the polymer film are investigated with X-ray photoelectron spectroscopy (XPS), atomic force microscopy (AFM), and scanning electron microscopy (SEM). The corrosion behavior of the coated NiTi and bare NiTi samples is compared by polarization test and electrochemical impedance spectroscopy (EIS) in simulated body fluid. The results show that the polymeric film lowers the corrosion current density and increases the polarization resistance, indicating improved corrosion resistance. The plasma polymerized coating is expected to reduce corrosion risks of biomedical NiTi alloy in clinical use.

1. Introduction

Biomedical shape memory nickel titanium (NiTi) alloys are widely used in biomedical devices and components due to the excellent shape memory effect and other desirable properties such as relatively low elastic modulus, good fatigue strength, and formability as well as super-elasticity [1]. However, long-term clinical use of NiTi alloys *in vivo* is still problematic because corrosion can lead to release of harmful nickel into body fluids and tissues subsequently causing severe cellular inflammation as well as toxic and allergic reactions in some patients [2,3].

Surface modification plays a vital role in improving the corrosion resistance of NiTi alloys. Laser oxidation [4], ion implantation [5,6], and thermal treatment [7] have been applied in the past years. Recently, surface plasma polymerization has received more attention because polymer films friendly to the human body can be produced by this means. Moreover, it is a versatile technique to prepare a homogeneous and pinhole free film with good surface coverage [8]. Precursors like allylamine and acryl acid have been employed to form plasma polymerized films with the desirable functional groups on metallic materials [9,10]. But, so far most researches focus on the biocompatibility of the polymer films and the corrosion protection offered by the coatings has seldom been reported. In this work, biomedical NiTi alloy is coated by plasma-polymerized allylamine (PPAAm) films and its corrosion resistance is investigated in simulated body fluids.

2. Experimental details

NiTi alloy plates (50.8 at% Ni) with dimensions of 10 mm × 10 mm × 2 mm were mechanically ground by SiC sandpaper to grade 1200, ultrasonically cleaned with acetone and deionized water, and then air dried. The plasma polymerized allylamine (PPAAm) films were deposited onto the NiTi substrates using capacitive plasma with standard 13.56 MHz excitation. Argon was used as the carrier gas and allylamine as the precursor gas. Prior to deposition, the NiTi substrates were cleaned by argon plasma sputtering for 10 min. Afterwards, allylamine was introduced into the chamber together with argon and polymerization was carried out at a pressure of 6 Pa and 30 W RF (radio frequency) power. Deposition was conducted for 10 min at room temperature.

X-ray photoelectron spectroscopy (XPS) with Al K_α irradiation was employed to determine the surface composition of the plasma polymerized film, and high-resolution spectra of the C1s, N1s, and O1s signals were recorded. The surface and cross-sectional morphology were examined by scanning electron microscopy (SEM). The surface topography and roughness were characterized using atomic force microscopy (AFM), and images were collected using the tapping mode from a sample size of $2 \times 2\ \mu m^2$. The electrochemical tests were performed on a Zahner

* Corresponding author.
E-mail address: paul.chu@cityu.edu.hk (P.K. Chu).

0167-577X/$ - see front matter © 2012 Elsevier B.V. All rights reserved.
http://dx.doi.org/10.1016/j.matlet.2012.08.054

Zennium electrochemical workstation using the three-electrode technique. The saturated calomel electrode (SCE) was the reference electrode and platinum sheet served as the counter electrode. The specimens with a surface area of $10 \times 10\ mm^2$ were exposed to a simulated body fluid (SBF) [11] and the tests were carried out at 37 °C. The polarization curves were acquired by scanning the potential at a rate of $1\ mV\ s^{-1}$ from -500 mV to 1200 mV. The EIS data at open-circuit potential were acquired over a frequency range of 10 mHz to 100 kHz with a sinusoidal perturbation potential amplitude of 10 mV.

3. Results and discussion

XPS is used to determine the surface chemical composition of the PPAAm film. The representative XPS wide scan spectrum and high-resolution C1s, N1s, and O1s spectra of the PPAAm film are depicted in Fig. 1. The C1s spectrum consists of three peaks: C1s I peak at 287 eV associated with imine (C═N) or nitrile (C≡N) groups, C1s II at 285.8 eV due to carbon atoms singly bonded to nitrogen (C–NH_2, C–NH–C, etc.), and C1s III peak at 284.6 eV corresponding to CH_x groups [12,13]. XPS also reveals oxygen incorporation into the films due to the non-ultra-high-vacuum (non-UHV) deposition conditions and exposure to air [14,15]. Hence, there may be overlapping peaks of C═O and C–O in the regions of C1s I and C1s II, respectively. During plasma polymerization, the gaseous organic precursors undergo ionization, fragmentation, and recombination processes on the substrate and the mechanism is typically quite complex [16]. Compared to the allylamine monomer, detection of N from the deposited film indicates retention of the amine groups. In addition, the smaller N/C ratio (16.7%) suggests that the mechanism may differ from that of the conventional polymer (repeating monomer units). More work is being conducted in this regard and new results will be promulgated in due course.

The SEM image in Fig. 2(a) shows the surface morphology of the coated PPAAm film and the thickness of the film (deposited a Si substrate under the same conditions) is determined to be around 300 nm from the cross-sectional image in the inset. The surface morphology of the bare and PPAAm coated NiTi alloy samples is depicted in the AFM images in Fig. 2(b) and (c). The results provide experimental evidence that plasma polymerization is a suitable technique to produce a uniform and smooth surface on NiTi [17].

Fig. 3(a) displays the polarization results of the uncoated NiTi alloy and PPAAm film coated NiTi alloy in SBF and the measured corrosion potential (E_{corr}) and corrosion current density (I_{corr}) are shown in Table 1. With the PPAAm coating, the whole

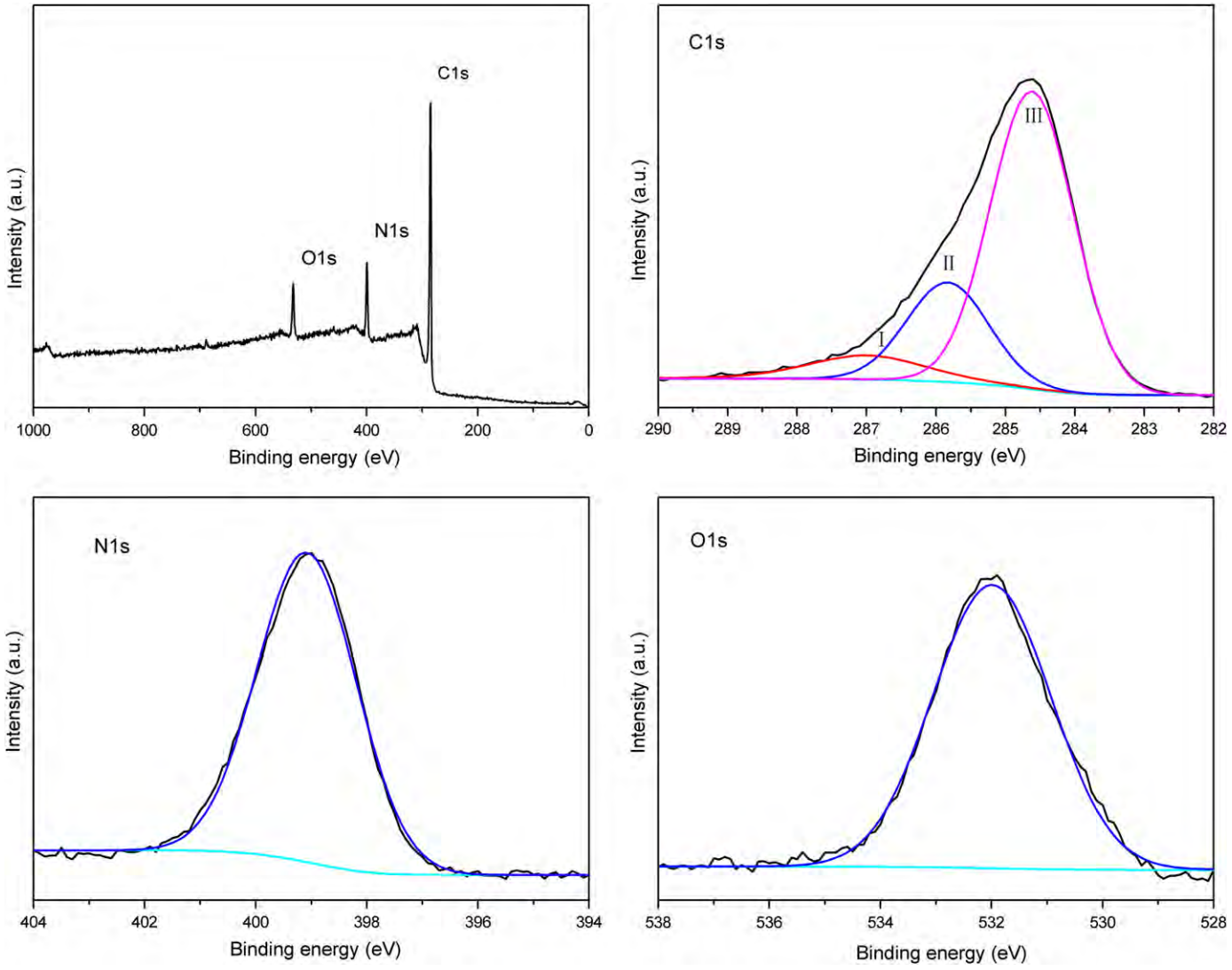

Fig. 1. Survey, C1s, N1s, and O1s spectra of PPAAm film deposited on NiTi substrate.

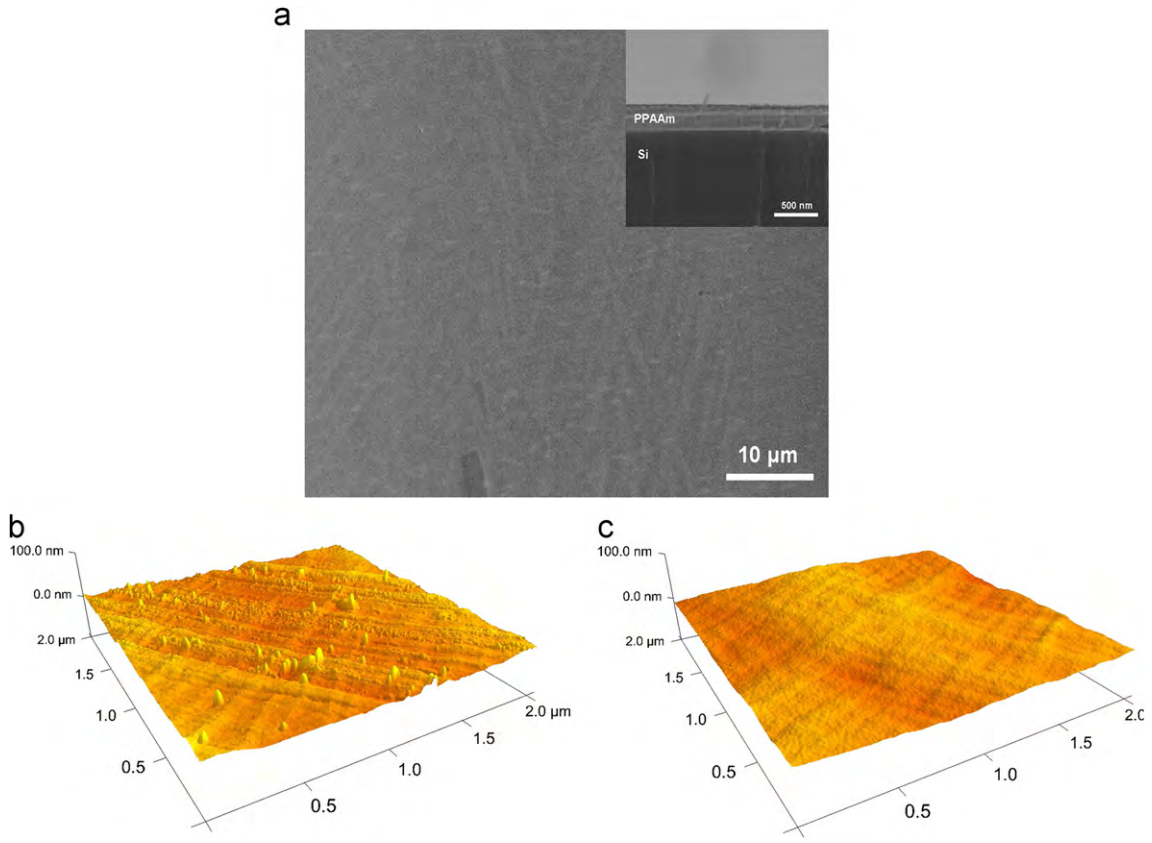

Fig. 2. (a) SEM image of PPAAm film (cross-section as inset). (b) and (c) AFM images ($2 \times 2\ \mu m^2$) of the surface of bare and PPAAm coated NiTi, respectively.

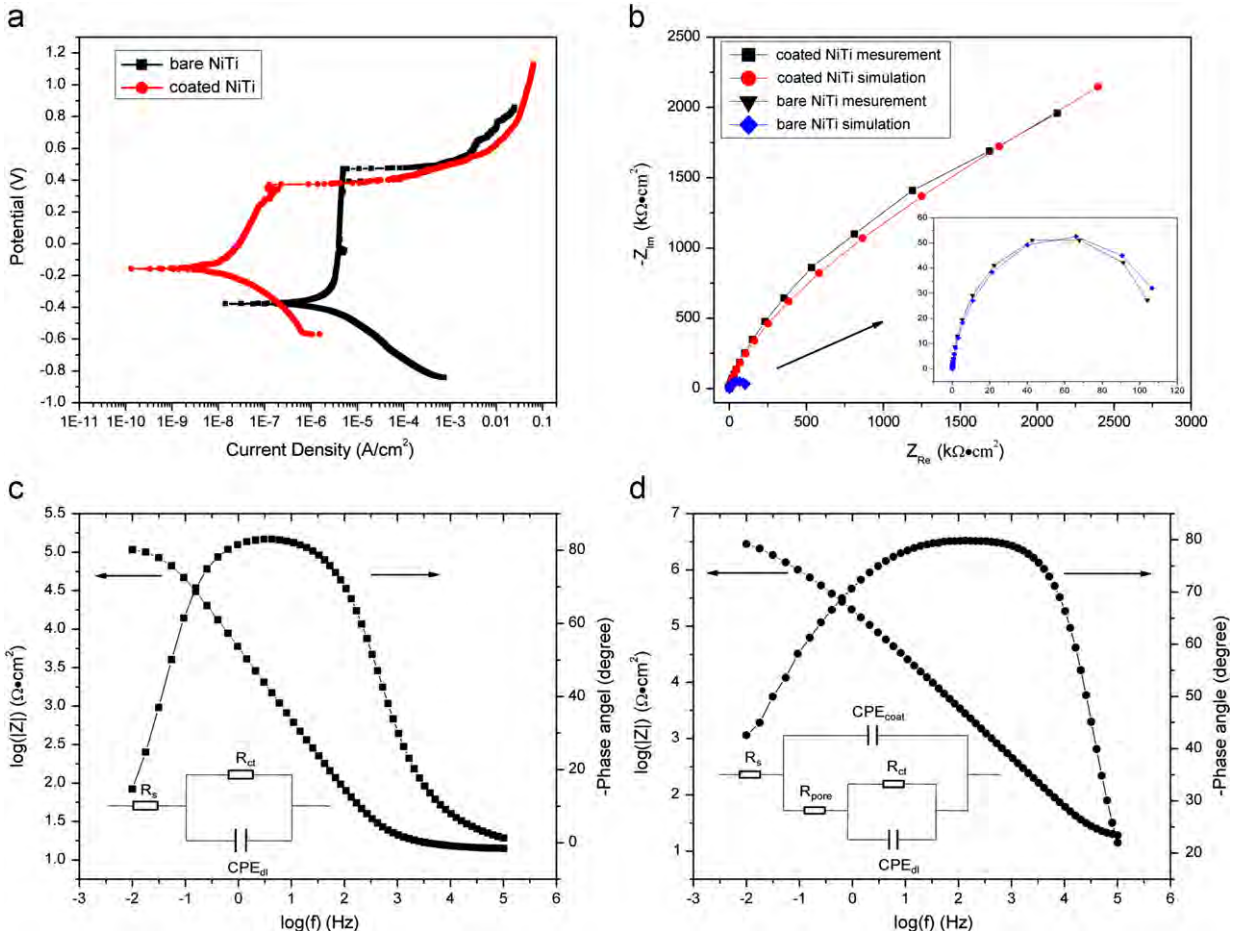

Fig. 3. (a) Polarization curves of bare NiTi and PPAAm film coated NiTi in SBF. (b) Measured and simulated Nyquist plots acquired in SBF. (c) Bode plots of bare NiTi with corresponding equivalent circuit. (d) Bode plots of PPAAm film coated NiTi with corresponding equivalent circuit.

Table 1
Parameters extracted from EIS and polarization tests in SBF.

Specimen	R_s	CPE_{coat}		R_{pore}	CPE_{dl}		R_{ct}	E_{corr}	I_{corr}
	($\Omega\,cm^2$)	($S\,cm^{-2}\,s^{-n}$)	n	($\Omega\,cm^2$)	($S\,cm^{-2}\,s^{-n}$)	n	($k\Omega\ cm^2$)	(mV)	($\mu A\,cm^{-2}$)
Bare NiTi	15.35	–	–	–	3.27×10^{-5}	0.91	121.2	−377	2.42
Coated NiTi	3.425	7.22×10^{-7}	0.36	13.17	7.98×10^{-7}	0.90	3.554×10^{12}	−156	0.0228

polarization curve shifts towards the region of lower current density and higher potential, indicating improved corrosion resistance. The corrosion potential and corrosion current density are -0.377 V and 2.42×10^{-7} A/cm^2 for the uncoated sample and -0.156 V and 2.28×10^{-8} A/cm^2 for the coated sample, respectively.

The EIS results at OCPs, shown in Fig. 3(b)–(d) as Nyquist and Bode plots with the corresponding equivalent circuit inset, impart important information about the corrosion behavior of the coated and uncoated samples. A significant larger capacitive loop arc in the Nyquist plots (Fig. 3(b)) confirms the improved corrosion resistance of the NiTi alloy with the PPAAm film. Fig. 3 (c) and (d) shows the corresponding equivalent circuits based on the EIS data. In this model, R_s is the resistance of the electrolyte between the working and reference electrodes, R_{ct} corresponds to the charge transfer resistance related to the electrochemical reaction, and R_{pore} is the pore resistance of the surface film [18]. CPE_{coat} and CPE_{dl} are the capacitances represented by the constant-phase elements (CPE), a substitution for ideal capacitor. CPE_{coat} represents the capacitance of the PPAAm film whereas CPE_{dl} is the capacitance at the substrate/electrolyte interface. The parameters associated with the equivalent circuits are listed in Table 1. The polarization resistance ($R_{ct}+R_{pore}$) increases significantly from $1.21\times10^5\,\Omega\,cm^2$ for the uncoated sample to $3.55\times10^{15}\,\Omega\,cm^2$ for the PPAAm coated sample, indicating a large improvement in the corrosion protection rendered by the polymer coating.

4. Conclusion

Uniform polymeric allylamine films are deposited onto NiTi by plasma polymerization. The corrosion behavior of the bare and PPAAm coated NiTi alloy samples in simulated body fluid is studied and compared. The coated sample shows a uniform and flat surface morphology, and both the polarization and EIS results demonstrate improved corrosion resistance in simulated body fluid. The polymer coated NiTi is expected to reduce corrosion risks in clinical use.

Acknowledgments

The work was supported by City University of Hong Kong Applied Research Grant (ARG) no. 9667066, Hong Kong Research Grants Council (RGC) General Research Funds (GRF) no. CityU 112510 and National Natural Science Foundation of China (NSFC) no. 51101053.

References

[1] Liu XY, Chu PK, Ding CX. Mater Sci Eng R 2004;47:49–121.
[2] Hart AJ, Quinn PD, Sampson B, Sandison A, Atkinson KD, Skinner JA, et al. Acta Biomater 2010;6:4439–46.
[3] Caicedo M, Jacobs JJ, Reddy A, Hallab NJ. J Biomed Mater Res A 2008;86:905–13.
[4] Wong MH, Cheng FT, Man HC. Mater Lett 2006;61:3391–4.
[5] Tan L, Dodd RA, Crone WC. Biomaterials 2003;24:3931–9.
[6] Gorji MR, Sanjabi S. Mater Lett 2012;73:179–82.
[7] Michiardi A, Aparicio C, Planell JA, Gil FJ. Surf Coat Technol 2007;201:6484–8.
[8] Yin Y, Wise SG, Nosworthy NJ, Waterhouse A, Bax DV, Youssef H, et al. Biomaterials 2009;30:1675–81.
[9] Seo HS, Ko YM, Shim JW, Lim YK, Kook JK, Cho DL, et al. Appl Surf Sci 2010;257:596–602.
[10] Yang Z, Wang J, Luo R, Maitz MF, Jing F, Sun H, et al. Biomaterials 2010;31:2072–83.
[11] Liu C, Xin Y, Tian X, Zhao J, Chu PK. J Vac Sci Technol A 2007;25(2):334–9.
[12] Beck AJ, Whittle JD, Bullett NA, Eves P, Mac Neil S, McArthur SL, et al. Plasma Process Polym 2005;2:641–9.
[13] Hamerli P, Weigel T, Groth T, Paul D. Biomaterials 2003;24:3989–99.
[14] Tatoulian M, Brétagnol F, Arefi-Khonsari F, Amouroux J, Bouloussa O, Rondelez F, et al. Plasma Process Polym 2005;2:38–44.
[15] Gancarz I, Bryjak J, Bryjak M, Tylus W, Poźniak G. Eur Polym J 2006;42:2430–40.
[16] Friedrich J. Plasma Process Polym 2011;8:783–802.
[17] Shi FF. Surf Coat Technol 1996;82(1–2):1–15.
[18] Wu G, Shanaghi A, Zhao Y, Zhang X, Xu R, Wu Z, et al. Surf Coat Technol 2012;206(23):4892–8.